# Comparisons of linear single-fluid MHD magnetic field line trajectories in DIII-D and NSTX-U during 3D magnetic perturbations

W. Wu[1], T. E. Evans[1], G. P. Canal[1], N. Ferraro[2], B. C. Lyons[3], D. Orlov[4], and X. Zhao[5]

[1]*General Atomics, PO Box 85608, San Diego, California 92186-5608, USA*

[2]*Princeton Plasma Physics Laboratory, Princeton, NJ 08541, USA*

[3]*Oak Ridge Associated Universities, Oak Ridge, TN 37831, USA*

[4]*Center for Energy Research, University of California San Diego, 9500 Gilman Dr., La Jolla, California 92093-0417, USA*

[5]*University of California San Diego, 9500 Gilman Dr., La Jolla, California 92093-0417, USA*

## I. Introduction

One typical DIII-D ELM suppressed shot for the RMP produced by the DIII-D I-coils configured for strongly resonant $n$ = 3 operations is analyzed in this paper. We present vacuum solutions from EFIT [1] and linear M3D-C[1] single-fluid MHD solutions [2] with axisymmetric vacuum field and 3D plasma response perturbation. We also present a NSTX-U case with $n$ = 3 perturbation for comparison and to investigate the impact of machine parameters, e.g. aspect ratio ($A$), normalized beta ($b_N$), and $q_{95}$ during future studies.

## II. TRIP3D-GPU field line integration accuracy test

TRIP3D-GPU [3], a parallelized version of the TRIP3D field line integration code [4], is used to analyze the magnetic field line trajectories. TRIP3D-GPU integrates a set of nonlinear magnetic field line differential equations, with its accuracy primarily dependent upon the poloidal position ($r$, $\theta$) of the magnetic field line, the toroidal angle step size ($\Delta\phi$), and the fidelity of magnetic field representation. To characterize the field line integration accuracy, we define the difference between the normalized magnetic flux of the i$^{th}$ step, $\Psi_i$, and its predecessor, $\Psi_{i-1}$, as the relative error, $RE_i = |\Psi_i - \Psi_{i-1}|$. Ideally, $RE_i$ should remain zero when tracing in the equilibrium-only magnetic field.

The accuracy when tracing an axisymmetric equilibrium as calculated by EFIT and the same equilibrium as calculated by M3D-C[1] is compared in Fig. 1. The DIII-D equilibrium is reconstructed from shot 147170 at time slice 3745 ms with $I_p$ = 1.60 MA, $B_T$ = 2.0 T, $q_{95}$ = 3.4, $A$ = 3.0 and $b_N$ = 1.8 [5]. The NSTX-U case is based on a model equilibrium, i.e., not an actual plasma discharge, and has $I_p$ = 1.45 MA, $B_T$ = 1.0 T, $q_{95}$ = 8.7, $A$ = 1.9 and $b_N$ = 4.0.

Magnetic field lines from five magnetic flux surfaces, namely at $\Psi$ = 0.5, 0.75, 0.93, 0.97, and $q$ = 3, were traced with toroidal angle step sizes $\Delta\phi$ ranging from 0.001° to 4.0° in

TRIP3D-GPU for this accuracy test. Each field line traverses more than one poloidal turn with $RE_{max} = \max(RE_i)$ recorded. In reality, $\Delta\phi$ is rarely chosen to be greater than 1.0° due to the concern of numerical accuracy. In fact, we typically limit $\Delta\phi$ to between 0.001° and 1.0° to compromise between accuracy and computational time. Therefore, in Fig. 1 data points with $\Delta\phi > 1.0°$ are marked with hollow symbols for information only. For each $\Delta\phi$, $RE_{max}$ typically becomes larger when tracing magnetic field lines closer to the plasma edge due to the curvature of local magnetic field.

In all four cases in this log-log chart, $RE_{max}$ can be fitted and bounded by a band expressed as $\Delta\phi^a/10^{b\pm c}$. As M3D-C$^1$ utilizes a finer computational mesh and a high-order finite-element representation of the magnetic field, the M3D-C$^1$ field generally produces more accurate tracing results than EFIT from large $\Delta\phi$ down until $RE_{max}$ saturates to a level at $\Delta\phi \sim 0.5°$. EFIT, however, utilizes a bicubic interpolation, whose $RE_{max}$ in principle decreases monotonically with $\Delta\phi$. In the expression of $\Delta\phi^a/10^{b\pm c}$, $a$ is a parameter of particular interest and likely dependent on the computational mesh configuration and data interpolation method, which controls the accuracy of approximating curves with straight lines. $a$ is found to be approximately equal to 2 for EFIT and 3.3 for M3D-C$^1$.

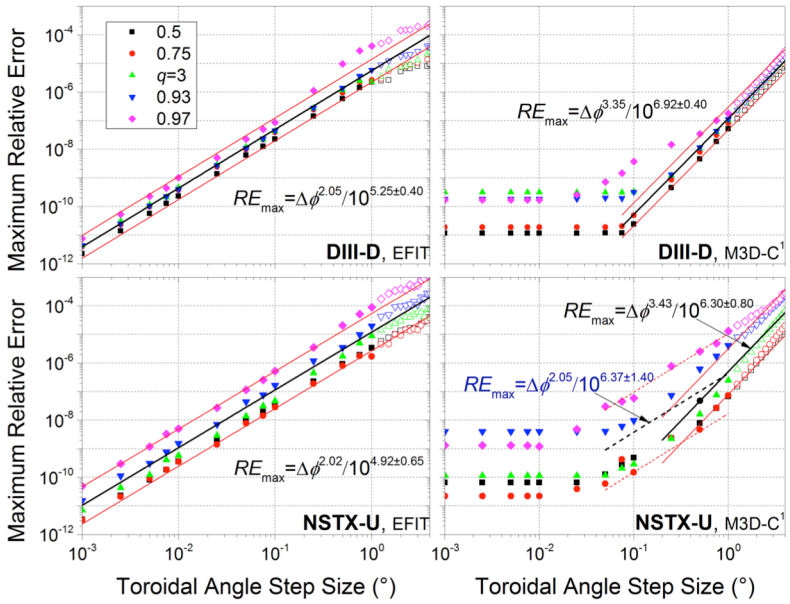


Fig. 1. Maximum relative error as a function of the toroidal step size used to trace magnetic field lines in five different magnetic flux surfaces: 0.5, 0.75, $q$=3, 0.93, and 0.97

The local mesh quality especially at the boundary can impact magnetic field line tracing accuracy, as it is evidenced by $RE_{max}$ at $\Psi = 0.97$, which is floating outside the band for EFIT at $0.25° \le \Delta\phi \le 1.0°$ for both machines, and for the M3D-C$^1$ field at $0.05° \le \Delta\phi \le 0.75°$ in DIII-D. The M3D-C$^1$ mesh for NSTX-U seems to be a special case since all field lines are showing the same deviation. In the typical working range with $0.1° \le \Delta\phi \le 1.0°$, $a$ is correlated to be 2.05 with a fairly large band width $c$, which suggests that this NSTX-U solution may be further improved by applying a better-quality M3D-C$^1$ mesh. Nevertheless,

for all different cases, $RE_{max}$ remains below $10^{-4}$, which corresponds to approximately 0.1 mm spatial difference. Therefore, by setting $\Delta\phi < 1.0°$ the accuracy of TRIP3D-GPU field line integration should be sufficient for interpreting the impact of plasma response.

**III. Physics interpretation on DIII-D and NSTX-U solutions**

Figure 2 shows the Poincaré plots of the 9/3 islands for DIII-D with 4 kA RMP I-coil fields, with top and bottom subfigures being the M3D-C$^1$ vacuum (initial condition) and single-fluid M3D-C$^1$ plasma response, respectively. Noticing the difference in the y-axis scales, these results indicate that the plasma screening effect not only significantly reduces the island size but also modifies the poloidal location of the islands.

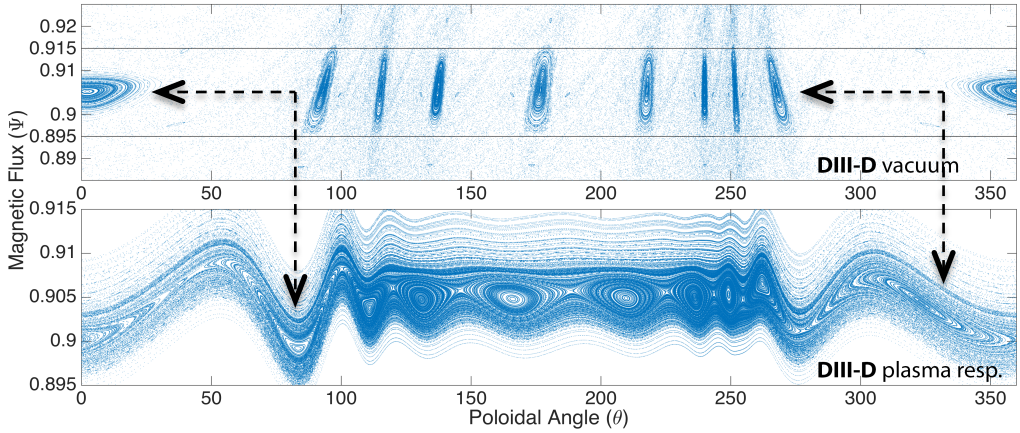


Fig. 2. Poincaré plot for $m/n$ = 9/3 islands in DIII-D discharge 147170 at 3745 ms; top: M3D-C$^1$ vacuum field, bottom: single-fluid M3D-C$^1$ plasma response

Figure 3 shows the Poincaré plots of the 9/3 island for NSTX-U, with the top and bottom subfigures being the M3D-C$^1$ vacuum (initial condition) and M3D-C$^1$ plasma response, respectively. Plasma screening modifies the location of magnetic islands and reduces the island size. Furthermore, in the center of the 9/3 perturbations we see a splitting that results in 18/6 islands that are not observed in the DIII-D case.

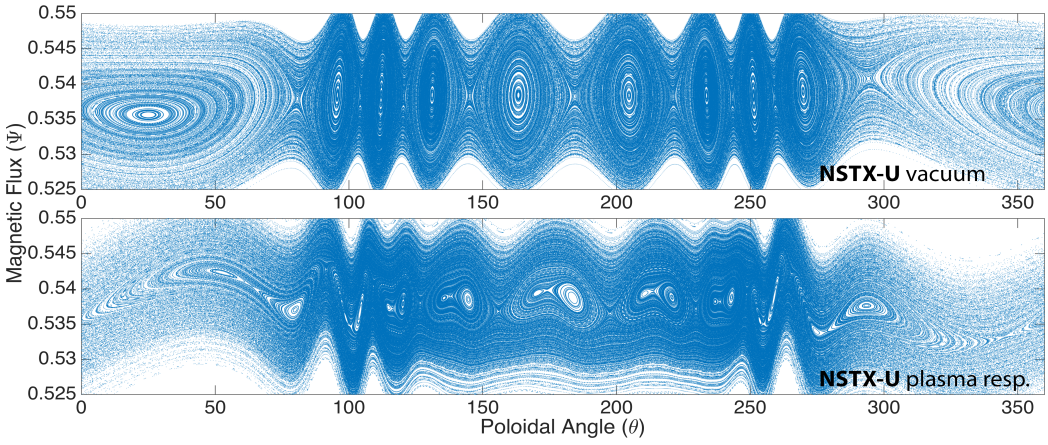


Fig. 3. Poincaré plot for NSTX-U; top: M3D-C$^1$ vacuum field, bottom: single-fluid M3D-C$^1$ plasma response

In comparing the vacuum versus plasma response, we observe that there are two competing factors which are the screening factors and the kink effect. By taking $\Delta\Psi_{\mathrm{vac}}/\Delta\Psi_{\mathrm{p.res}}$ for the largest island for both machines, where $\Delta\Psi$ is the difference between the maximum and minimum $\Psi$ of the islands, the screening factors are found to be 3.83 and 2.20 for DIII-D and NSTX-U, respectively. In comparison to the 9/3 islands in DIII-D, the kink effect for NSTX-U is observed to be less significant, as evidenced by the DIII-D islands at 2.23° and 268.08°, which show large distortion and displacements in $\Psi$. This is likely due to the fact that the kink response is typically found to be stronger near the edge of the plasma and NSTX-U is operating at higher edge safety factor so the $q$ = 3 surface is deeper into the plasma. The kink effect can be influenced by the shaping of the plasma, which is currently being investigated.

## IV. Conclusion

The numerical accuracy of EFIT and M3D-C[1] solutions are demonstrated in this paper when studying the $n$ = 3 magnetic perturbations in DIII-D and NSTX-U with TRIP3D-GPU. In comparing DIII-D and NSTX-U cases, we conclude that difference in machine parameters can significantly impact plasma response. Kink effects and plasma screening reduce, distort, or shift islands in both machines substantially. We attempt to eventually identify the impact of each individual plasmas parameters such as aspect ratio ($A$), normalized beta ($b_{\mathrm{N}}$), and $q_{95}$.

## Acknowledgements

This material is based upon work supported by the U.S. Department of Energy, under awards DE-FC02-04ER54698[1], DE-FC02-04ER54861[1], DE-AC02-09CH11466[2], and DE-FG02-05ER54809[4]. DIII-D data shown in this paper can be obtained in digital format by following the links at https://fusion.gat.com/global/D3D_DMP.

## References

1. L.L. Lao, et. al., Nucl. Fusion 30 (1990) 1035
2. N. Ferraro, et al., Nucl. Fusion 53 (2013) 073042
3. R.C. Kalling, et al., Fus. Eng. Design 86 (2011) 399-406
4. T. E. Evans, et. al., Phys. Plasmas 9 (2002) 4957
5. T. E. Evans, Plasma Phys. Contr. F. 57 (2015) 123001